Heliyon 11 (2025) e40146

Contents lists available at ScienceDirect

Heliyon

journal homepage: www.cell.com/heliyon

Research article

Optimization of regions of interest sampling strategies for proton density fat-fraction MRI of hepatic steatosis before liver transplantation in ex vivo livers

Gen Chen, Hao Tang, Yang Yang, Lifen Zhou, Qiuxia Wang *, Daoyu Hu, Zhen Li

Department of Radiology, Tongji Hospital, Tongji Medical College, Huazhong University of Science and Technology, 1095 Jiefang Avenue, Qiaokou District, Wuhan, 430030, Hubei, China

ARTICLE INFO

Keywords:
Hepatic steatosis
Sampling strategy
Liver transplantation
Proton density fat fraction

ABSTRACT

Objectives: The quantity of regions of interest (ROIs) constitutes the primary determinant of the time investment in image analysis. In the context of proton density fat-fraction (PDFF) magnetic resonance imaging (MRI) conducted on liver grafts in ex vivo conditions, this research systematically examines various ROI sampling strategies. The findings of this study furnish essential insights, offering a foundation for optimizing time efficiency while ensuring precise assessment of hepatic steatosis before the crucial process of liver transplantation.

Methods: This was a retrospective analysis of a prospective study and included 35 liver grafts with histopathological steatosis that underwent 3T PDFF MRI in ex vivo. One ROI of 1 cm^2 was selected for each hepatic segment, and any combination of ROIs in 1–8 liver segments was used, resulting in 511 combinations. Using intraclass correlation coefficients (ICCs) and Bland-Altman analyses, the PDFFs of all these combinations were compared with the 9-ROI average PDFF. There was a moderate correlation between the average PDFF and the histological findings ($R = 0.47$, $P < 0.01$).

Results: The average 9-ROI PDFF of all liver grafts was 4.07 ± 4.35 % (0.870–20.904). All strategies with ≥5 ROIs had intraclass correlation coefficient (ICC) ≥ 0.995 and absolute limits of agreement (|LOA|)≤ 1.5 %. Overall, 54 of 84 (67.5 %) 3-ROI sampling strategy had ICC ≥0.995, and 70 of 84 (70 %) had |LOA|≤ 1.5 %. A total of 111 of 126 (88.1 %) 4-ROI sampling strategy had ICC ≥0.995, and 125 of 126 (99.2 %) had |LOA| ≤ 1.5 %.

Conclusions: The employment of the 5-ROI sampling strategy proves instrumental in both time conservation and precise assessment of hepatic steatosis within liver grafts during the ex vivo phase preceding liver transplantation.

1. Introduction

Hepatic steatosis, characterized by the accumulation of triglycerides in hepatocyte cytoplasm, is a prevalent condition globally [1, 2]. Due to the shortage of donor organs and the utilization of marginal donors, livers exhibiting hepatic steatosis are increasingly considered for transplantation [3]. It is crucial to recognize that hepatic steatosis constitutes a critical risk factor during and post liver

* Corresponding author.
E-mail addresses: genchen@hust.edu.cn (G. Chen), haotangtjh@126.com (H. Tang), yangyangaddress@163.com (Y. Yang), zhoulifen1976@163.com (L. Zhou), wangqiuxia@hust.edu.cn (Q. Wang), jr.hudaoyu@vip.163.com (D. Hu), zhenli@hust.edu.cn (Z. Li).

https://doi.org/10.1016/j.heliyon.2024.e40146
Received 21 November 2023; Received in revised form 15 February 2024; Accepted 4 November 2024
Available online 19 November 2024

surgery, exerting a significant impact on patient prognosis following transplantation [4–6]. Typically, surgeons employ visual inspection as an evaluative tool for hepatic steatosis during donor surgery, a method that inherently bears potential for error and subjectivity. Although liver biopsy remains the gold standard for hepatic steatosis diagnosis, it poses invasiveness and substantial sampling variability concerns [7,8].

Proton density fat fraction MRI (PDFF MRI) represents a chemically encoded magnetic resonance imaging technique utilizing the quantitative biomarker PDFF to assess liver fat content. Numerous investigations have employed PDFF MRI as a reliable biomarker for hepatic steatosis and for monitoring the outcomes of treatment interventions [9–14]. Notably, the majority of cadaveric organ donors have not undergone pre-donation MR evaluation. However, recent studies have affirmed PDFF as a viable ex vivo imaging biomarker for the assessment of hepatic steatosis [15–17].

The heterogeneous distribution of hepatic fat necessitates the consideration of diverse techniques for the accurate placement of regions of interest (ROIs) within the liver, potentially resulting in variations in the quantification of fat content [18–20]. In previous studies, our research has demonstrated the utility of volumetric quantitative PDFF MRI histogram analysis as a valuable non-invasive method for detecting macrovesicular hepatic steatosis in ex vivo conditions before liver transplantation [21]. However, it is noteworthy that this approach is time-intensive. Conventionally, one ROI is placed in each hepatic segment [22,23] and the quantity of ROIs significantly influences the duration of image analysis. Recent findings by Campo et al. emphasize that an increase in both the number and size of ROIs imposes a greater time burden on radiologists for liver PDFF measurement [24]. T Consequently, there is a pressing need to develop a sampling strategy that is both time-efficient and accurate for measuring liver PDFF prior to liver transplantation.

In the context of PDFF MRI conducted on liver grafts ex vivo, this study systematically examines strategies related to ROI sampling. The research findings offer valuable insights into optimizing time efficiency while ensuring precise evaluation of hepatic steatosis before the critical procedure of liver transplantation.

2. Materials and methods

2.1. Liver grafts

This study constitutes a retrospective secondary analysis involving 35 liver grafts exhibiting histopathological macrovesicular hepatic steatosis, which were subjects of 3T MRI within the framework of a prior prospective study. The cadaveric human livers utilized in this research were sourced from organ donation after citizen death and were obtained through the hospital's organ procurement organization, with due authorization for their application in clinical practice, educational endeavors, and scientific investigations. Preceding this study, the cadaveric livers had undergone visual inspection, biopsy, and histological evaluation, procedures carried out by the surgeon and pathologist. Prior to donation, the liver was devoid of any underlying hepatic diseases.

2.2. MRI acquisition

MRI was performed using a 3T system (Discovery MR750, GE Healthcare). Routine liver protocols with the heart coil (16-channel torso array coil) were carried out. Surgeons preserved all liver grafts in the University of Wisconsin solution and ice-water mixture in the container, which is standard practice for routine organ transplantation. The containers with the liver grafts were then transferred to the MR scanning room. PDFF MRI was performed using the parameters listed in Table S1.

2.3. Image analysis

All MR images were reviewed by two radiologists who had 7 and 13 years of experience, respectively, in abdominal MRI and were blinded to the clinical details. Because the FatFrac image does not clearly delineate the anatomy, we placed one ROI in each Couinaud liver segment, referencing the R2*, water, and T2-weighted images to avoid blood vessels, bile ducts, and artifacts. The area of each ROI was approximately 1 cm^2 [20]. We recorded the PDFF values for each segment of each liver graft.

2.4. ROI sampling strategies

Various configurations of one to eight ROIs within liver segments were employed in our analysis, yielding a total of 511 distinct combinations. To assess the consistency of these combinations, intraclass correlation coefficients (ICCs) and Bland-Altman analyses were conducted, comparing the PDFFs derived from these configurations with the PDFF obtained from the averaged data of nine ROIs within the liver grafts. For our evaluation, a threshold of ICC $\geq$0.995 and an absolute limit of agreement (LOA) $\leq$ 1.5 % were established as criteria for close agreement. Such agreements were considered clinically meaningful, signifying negligible differences [25].

2.5. Visual inspection assessment

The surgeon conducted a qualitative assessment of the liver grafts utilizing direct observational methods and documented on a scale, with designations of 'normal', 'mild/moderate', and 'severe', which were quantitatively represented by visual scores of 3, 2, and 1, in respective order.

2.6. Histological assessment

A uniform tissue sample, measuring approximately 0.5 × 0.5 × 0.5 cmˆ3, was meticulously excised from the hepatic surface by means of a surgical scalpel. Subsequent to excision, the specimen underwent fixation in a formalin solution and was subjected to staining procedures utilizing hematoxylin and eosin for routine histological examination. According to the histological evaluation, the 35 liver grafts were divided into two groups: normal group (Grade 0) and macrovesicular hepatic steatosis group (Grade 1, 2, 3, and 4).

2.7. Statistical analysis

Descriptive statistics, including means and standard deviations (±SD), were employed to characterize continuous variables in this study. Statistical analyses were conducted using R software, version 3.6.1. A significance threshold was established at a level of $P < 0.05$, denoting statistical significance.

Interobserver reproducibility was assessed through ICC, with a value exceeding 0.80 denoting excellent reproducibility between observers. To explore the relationship between histological hepatic steatosis and PDFF, linear regression analysis was employed. Depending on the data distribution, Pearson or Spearman correlation coefficients were utilized to investigate potential correlations between average or segmental PDFF values and histological findings. Moderate correlation refers to a certain degree of relationship between two variables, with the correlation coefficient falling within a moderate range. For instance, correlation coefficients ranging from −0.3 to −0.8 or from +0.3 to +0.8 are typically considered as moderate correlations.

3. Results

3.1. Donor characteristics

We conducted an analysis encompassing 35 liver grafts derived from 30 male and 5 female patients, each of which underwent histological assessments, as illustrated in Fig. 1. The patients exhibited a mean body mass index of 22.20 ± 2.32 kg/m^2, with a mean age of 43.40 ± 10.84 years. Furthermore, their mean aspartate aminotransferase level was 56.08 ± 47.83 U/L, and the mean total bilirubin level was 12.45 ± 11.04 U/L. Surgeons, based on visual assessment, assigned a mean score of 2.00 ± 0.91 (Table 1). An illustrative representation of typical findings is depicted in Fig. 2. The visual score in the macrovesicular steatosis group was higher than that in the normal group ($P = 0.004$).

3.2. Interobserver agreement of PDFF

The interobserver agreement, as indicated by the ICC exceeding 0.80 for segmental PDFFs as outlined in Table S2, demonstrated a level of excellence. Consequently, the measurements obtained from the second radiologist were utilized for our analysis.

3.3. PDFF of liver segments

The mean PDFF derived from the average of 9-ROI across all liver grafts was 4.07 ± 4.35 % (ranging from 0.870 % to 20.904 %), as presented in Table 2. Segment III exhibited the highest mean PDFF value at 4.35 %, surpassing the 9-ROI average by 0.28 %. Conversely, segment II demonstrated the lowest mean PDFF value at 3.78 %, indicating a 0.29 % deviation from the 9-ROI average. However, no statistically significant disparities were observed in segmental PDFF values ($P > 0.05$). Moreover, no significant distinction was noted between the average PDFF of the left lobe (inclusive of the caudate lobe) and the right lobe (bias = −0.230, limits of agreement (LOA) = −2.067 to 1.608, $P = 0.156$), as depicted in Fig. 3. Nonetheless, in 11.4 % (4 out of 35) of the liver grafts, the

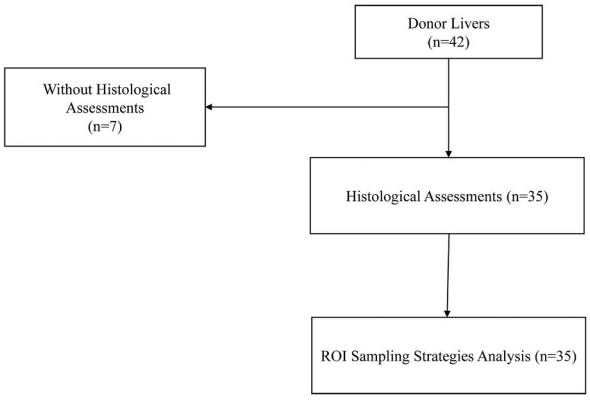

Fig. 1. Flowchart shows process of selecting liver grafts.

Table 1
Characteristics of clinical and laboratory.

Donor characteristics	All livers (n = 35)
Age (years)	43.40 ± 10.84
BMI[a]	22.20 ± 2.32
Sex	
Man	30
Woman	5
AST[b]	56.08 ± 47.83
ALT[c]	42.67 ± 35.98
ALB[d]	32.71 ± 7.21
TB[e]	12.45 ± 11.04
Visual score	2.00 ± 0.91

[a] Units of kg/m_2 for BMI.
[b] Units of U/L for AST.
[c] Units of U/L for ALT.
[d] Units of g/L for ALB.
[e] Units of umol/L for TB.

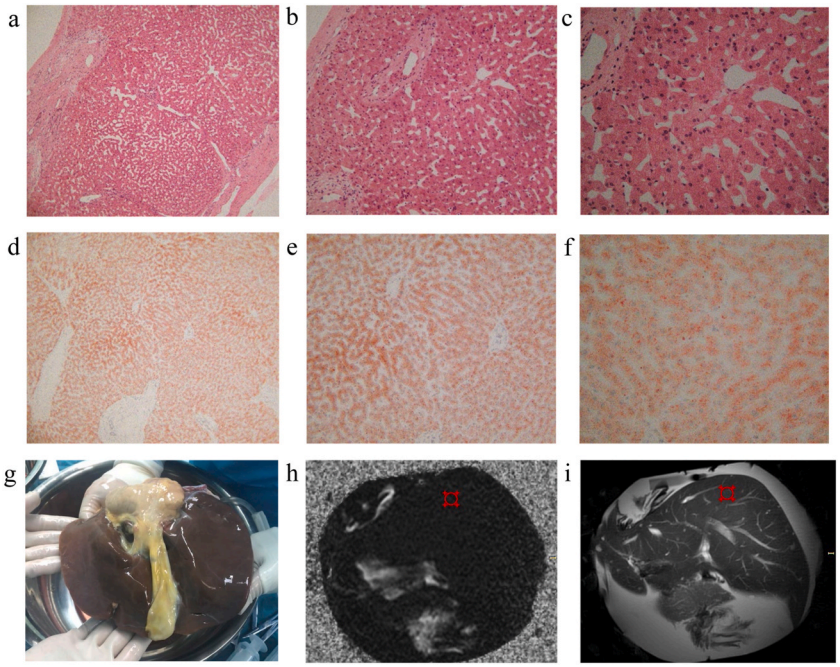

Fig. 2. Representative images of an 18-year-old man liver graft. (a–c) Pathology confirmed as macrovesicular hepatic steatosis (hematoxylin and eosin; original magnification,×100, × 200 and × 400, respectively); (d–f) Oil red staining confirmed as macrovesicular hepatic steatosis (original magnification,×100, × 200 and × 400, respectively); (g) Visual inspection; (h) ROI of the liver on FatFrac image of IDEAL-IQ; (i) ROI of the liver on T2-weighted image.

PDFF disparity between the left and right liver lobes exceeded 1.5 %. A moderate correlation was established between the average PDFF values and histological findings ($R = 0.47$, $P < 0.01$).

3.4. ICC analysis

Our findings revealed a positive correlation between the ICC and the number of ROIs utilized, as illustrated in Fig. 4. Among the sampling strategies employing a single ROI, all exhibited an ICC value below 0.995. Conversely, among the 36 strategies utilizing two ROIs, 11.1 % (4 out of 36) demonstrated an ICC value equal to or exceeding 0.995. In the case of strategies involving three ROIs, 67.5 % (54 out of 84) displayed an ICC value of 0.995 or higher. This trend further intensified with an increase in the number of ROIs; specifically, 88.1 % (111 out of 126) of strategies with four ROIs, as well as all strategies employing five or more ROIs, exhibited an ICC equal to or surpassing 0.995, as detailed in Table 3.

Table 2
Mean PDFF values by hepatic segment.

Segment(s)	Mean PDFF(%)
I	3.84 ± 3.95
II	3.78 ± 4.20
III	4.35 ± 4.60
IVa	4.09 ± 4.46
IVb	3.81 ± 3.92
V	4.22 ± 4.46
VI	4.33 ± 5.02
VII	4.20 ± 4.73
VIII	4.06 ± 4.57
Whole liver (all segments)	4.07 ± 4.35

The lowest PDFF values were recorded in segment II and the highest PDFF values were recorded in segment III.
PDFF = proton density fat-fraction.

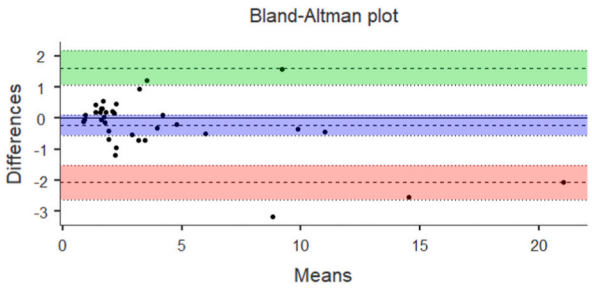

Fig. 3. Bland-Altman plot of the left and right lobe proton density fat-fraction values in the 35 liver grafts of this study.

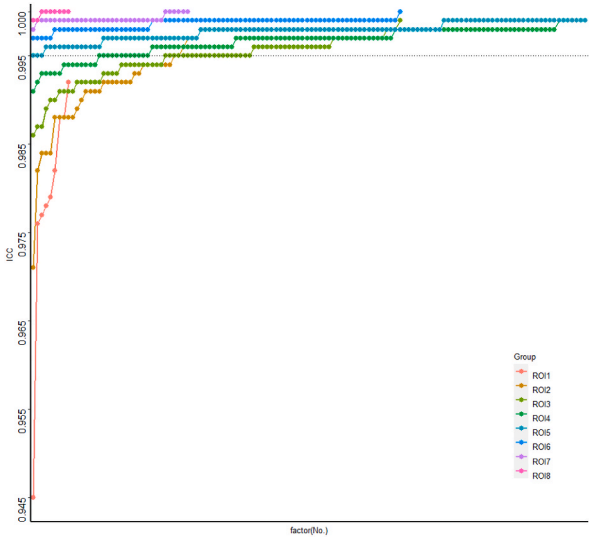

Fig. 4. The intraclass correlation coefficients (ICCs) (y-axis) for the different sampling strategies in relation to the number of ROIs (y-axis). Each dot represents a particular sampling strategy (511 in total). The ICC increased with the number of ROIs.

3.5. LOA analysis

An inverse relationship between the number of ROIs employed and the corresponding LOA was observed, as depicted in Fig. 5. Specifically, all sampling strategies utilizing a single ROI exhibited an absolute LOA (|LOA|) exceeding 1.5 %. In contrast, 70 % (70 out of 84) of the sampling strategies employing three ROIs had |LOA| values equal to or less than 1.5 %. Moreover, 99.2 % (125 out of 126) of strategies employing four ROIs, as well as all strategies utilizing five or more ROIs, demonstrated |LOA| values within the threshold of 1.5 %, as detailed in Table 4.

Table 3
ICCs bounds by number of ROIs.

Number of ROIs	Proportion with ICC ≥0.995	Average ICC	Lowest ICC	Highest ICC
1	0 % (0/9)	0.978	0.945	0.992
2	11.1 % (4/36)	0.991	0.971	0.997
3	67.5 % (54/84)	0.995	0.986	0.999
4	88.1 % (111/126)	0.997	0.991	0.999
5	100 % (126/126)	0.998	0.995	0.999
6	100 % (84/84)	0.999	0.997	1.000
7	100 % (36/36)	0.999	0.998	1.000
8	100 % (9/9)	1.000	0.999	1.000

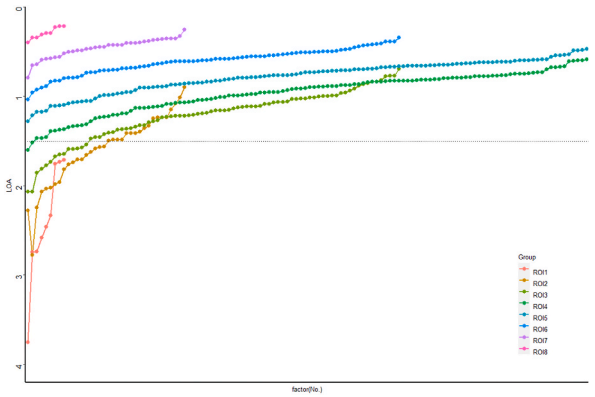

Fig. 5. Level of agreement (LOA) bounds (y-axis) shown for the different sampling strategies by the number of regions of interests (ROIs). Each dot represents a particular sampling strategy (511 in total). The LOA decreased as the number of ROIs per strategy increased.

3.6. Sampling strategies

In Fig. 4, it is evident that the ICCs associated with various ROI sampling strategies consistently increased with a rise in the number of ROIs. Simultaneously, as illustrated in Fig. 5, the LOAs for all ROI sampling strategies demonstrated a decline with an increase in the number of ROIs utilized. Sampling strategies in which the number of ROIs in the left and right liver lobes differed by no more than one were identified as balanced subsets. Detailed analysis, presented in Table S2, discerned these subsets and unbalanced subsets based on the proportion of cases exhibiting ICC values ≥ 0.995 and absolute LOA (|LOA|) values ≤ 1.5 %. The findings in Table S3 revealed that, in the case of 2-, 3-, and 4-ROI combinations, balanced sampling strategies were more likely to yield PDFF results similar to those obtained with the 9-ROI strategy. However, these outcomes were not consistently sustainable over time.

4. Discussion

Our study highlights that a minimum of five ROIs is essential to achieve comparable PDFF results as the 9-ROI strategy in ex vivo assessments of hepatic steatosis before liver transplantation. We observed that the use of a single ROI failed to yield satisfactory ICC or LOA. On the other hand, employing two, three, or four ROIs led to acceptable ICC and LOA values in specific instances. Notably, sampling strategies with a balanced subset, where the difference in the number of ROIs between the left and right liver lobes did not exceed one, exhibited a higher likelihood of producing PDFF results akin to the 9-ROI approach. However, this congruence was not consistently sustainable, potentially influenced by the uneven distribution of fat within the liver. Intriguingly, our study revealed no significant differences in segmental PDFF values. Segment III displayed the highest mean PDFF value, while segment II exhibited the lowest. Surprisingly, we found no notable disparity in the average lobar PDFF between the left lobe (including the caudate lobe) and the right lobe (bias = −0.230, limits of agreement (LOA) = −2.067 to 1.608, P = 0.156), as depicted in Fig. 3, which contrasts previous findings, notably those of Bonekamp et al., who observed differential fat content between the right and left liver lobes. In their study, segment II demonstrated the lowest segmental PDFF, whereas segment VIII exhibited the highest PDFF [18].

In the context of the 5-ROI strategy, our study identified that all 99 balanced and 27 unbalanced subsets exhibited satisfactory ICC and LOA. Previous research has underscored the enhanced correlation between sampling strategies that encompass multiple liver segments or ROIs from both liver lobes and the average PDFF, along with an improvement in the repeatability of PDFF measurements with an increase in the number of ROIs. However, it is crucial to note that the number of ROIs significantly impacts the time burden on radiologists [24,25]. Campo et al. demonstrated that as the number and size of ROIs increased, the time required for radiologists to measure PDFF also escalated [24]. Hong et al. discovered that a 4-ROI sampling strategy, with two ROIs in each lobe, closely aligned with PDFF values obtained from the 9-ROI strategy, indicating a notable agreement [25]. Additionally, Di Cao et al. recommended a

Table 4
LOA bounds by number of ROIs.

Number of ROIs	Proportion with |LOA| ≤ 1.5 %	Average |LOA|	Lowest |LOA|	Highest |LOA|
1	0 % (0/9)	2.424	1.710	3.752
2	50 % (18/36)	1.596	0.896	2.777
3	83.3 % (70/84)	1.220	0.690	2.070
4	99.2 % (125/126)	0.961	0.588	1.602
5	100 % (126/126)	0.776	0.47	1.281
6	100 % (84/84)	0.61	0.345	1.034
7	100 % (36/36)	0.295	0.214	0.400
8	100 % (9/9)	0.292	0.214	0.400

|LOA| refers to the highest absolute value of either side of the bound.

3L-ROI sampling strategy at the puncture site segment for hepatic PDFF, utilizing liver puncture biopsy as the gold standard. Their study emphasized that the PDFF measured by the subset of 3L-ROI at the puncture site segment most accurately reflected the liver biopsy results [26].

However, it is important to note that all the aforementioned strategies were employed in vivo settings. In our present ex vivo study, uniform-sized ROIs were utilized across all liver segments, and a minimum of five ROIs were necessary to achieve results comparable to those obtained with the PDFF measurement using the 9-ROI strategy.

In our investigation, the average PDFF exhibited a moderate correlation with the histological diagnosis. Previous in vivo studies have juxtaposed MRI-derived PDFF values with histological evaluations of biopsy samples. While these studies demonstrated varying results, MRI-derived PDFF exhibited a strong or very strong correlation with histological grading in some instances [15,27,28]. Small number of liver grafts and inherent variability in histological grading may contribute to the moderate correlation observed between the average PDFF and the diagnosis of macrovesicular hepatic steatosis in the histological examination.

This study's notable strength lies in the comprehensive evaluation of all conceivable ROI combinations. By establishing specific thresholds indicative of close agreement with the 9-ROI values, we identified highly effective sampling strategies utilizing five ROIs. This determination was facilitated by prior research demonstrating the enhanced reliability of results with an increased number of ROIs. It is imperative to emphasize that while these strategies were validated in vivo, swift and precise measurements before transplantation are paramount, underscoring the critical need for rapid and accurate assessment methodologies in clinical practice.

This study presents several noteworthy limitations. Primarily, our comparison was based on the 9- ROI sampling strategy, which, although widely utilized and accepted in numerous studies, lacks comprehensive validation. Moreover, the relatively small sample size of liver grafts in our study necessitates caution in generalizing our findings, highlighting the need for further extensive validation in larger cohorts. Additionally, our study employed uniform-sized ROIs, precluding an exploration of the impact of varying ROI sizes on the results. Previous in vivo studies with patients have indicated that larger ROIs tend to yield greater consistency in outcomes, indicating the significance of this parameter, which remains unexplored in our current study. Fourth, livers were scanned at low temperatures. Bias may be introduced under this condition. The PDFF of liver in our study may be lower than in vivo because the difference between regular transplant organ temperature and body temperature influences the fat fraction. Fifth, MRI-PDFF assessment of the liver was not directly compared between ex vivo and in vivo conditions. Therefore, further extensive investigations are necessary to address the aforementioned constraints and validate the findings of the present study.

5. Conclusion

Our study provides empirical evidence supporting the efficacy of the 5- ROI sampling strategy in expediting the evaluation process while ensuring accurate assessment of hepatic steatosis within liver grafts during the ex vivo phase before liver transplantation.

CRediT authorship contribution statement

Gen Chen: Writing – original draft, Visualization, Validation, Software, Methodology, Investigation, Formal analysis, Data curation, Conceptualization. **Hao Tang:** Validation, Software, Methodology. **Yang Yang:** Methodology. **Lifen Zhou:** Resources, Data curation. **Qiuxia Wang:** Writing – review & editing, Supervision, Project administration. **Daoyu Hu:** Writing – review & editing, Supervision, Project administration. **Zhen Li:** Writing – review & editing, Supervision, Resources, Project administration, Funding acquisition, Conceptualization.

Ethics statement

This work was approved by the Ethics Committee of the Medical Ethics Committee, Tongji Hospital, Tongji Medical College, Huazhong University of Science and Technology (TJ-IRB20181105).

Additional information

No additional information is available for this paper.

Funding statement

This study was supported by National Natural Science Foundation of China (82071889).

Declaration of competing interest

The authors have no conflicts of interest to declare.

Acknowledgements

We thank Changhua Wan, whose important contributions to this study were indispensable to its success.

Appendix A. Supplementary data

Supplementary data to this article can be found online at https://doi.org/10.1016/j.heliyon.2024.e40146.

References

[1] I. Linares, M. Hamar, N. Selzner, M. Selzner, Steatosis in liver transplantation: current limitations and future strategies, Transplantation 103 (2019) 78–90.
[2] J. Byun, S.S. Lee, Y.S. Sung, Y. Shin, J. Yun, H.S. Kim, E.S. Yu, S.G. Lee, M.G. Lee, CT indices for the diagnosis of hepatic steatosis using non-enhanced CT images: development and validation of diagnostic cut-off values in a large cohort with pathological reference standard, Eur. Radiol. 29 (2019) 4427–4435.
[3] M.J. Chu, A.J. Dare, A.R. Phillips, A.S. Bartlett, Donor hepatic steatosis and outcome after liver transplantation: a systematic review, J. Gastrointest. Surg. 19 (2015) 1713–1724.
[4] C. Flechtenmacher, P. Schirmacher, P. Schemmer, Donor liver histology–a valuable tool in graft selection, Langenbeck's Arch. Surg. 400 (2015) 551–557.
[5] A.L. Spitzer, O.B. Lao, A.A. Dick, R. Bakthavatsalam, J.B. Halldorson, M.M. Yeh, M.P. Upton, J.D. Reyes, J.D. Perkins, The biopsied donor liver: incorporating macrosteatosis into high-risk donor assessment, Liver Transplant. 16 (2010) 874–884.
[6] M. Fiorentino, F. Vasuri, M. Ravaioli, L. Ridolfi, W.F. Grigioni, A.D. Pinna, A. D'Errico-Grigioni, Predictive value of frozen-section analysis in the histological assessment of steatosis before liver transplantation, Liver Transplant. 15 (2009) 1821–1825.
[7] V. Ratziu, F. Charlotte, A. Heurtier, S. Gombert, P. Giral, E. Bruckert, A. Grimaldi, F. Capron, T. Poynard, Sampling variability of liver biopsy in nonalcoholic fatty liver disease, Gastroenterology 128 (2005) 1898–1906.
[8] D.E. Kleiner, E.M. Brunt, M. Van Natta, C. Behling, M.J. Contos, O.W. Cummings, L.D. Ferrell, Y.C. Liu, M.S. Torbenson, A. Unalp-Arida, M. Yeh, A. J. McCullough, A.J. Sanyal, Design and validation of a histological scoring system for nonalcoholic fatty liver disease, Hepatology 41 (2005) 1313–1321.
[9] J. Gu, S. Liu, S. Du, Q. Zhang, J. Xiao, Q. Dong, Y. Xin, Diagnostic value of MRI-PDFF for hepatic steatosis in patients with non-alcoholic fatty liver disease: a meta-analysis, Eur. Radiol. 29 (2019) 3564–3573.
[10] J.L. Rehm, P.M. Wolfgram, D. Hernando, J.C. Eickhoff, D.B. Allen, S.B. Reeder, Proton density fat-fraction is an accurate biomarker of hepatic steatosis in adolescent girls and young women, Eur. Radiol. 25 (2015) 2921–2930.
[11] X. Zhong, M.D. Nickel, S.A. Kannengiesser, B.M. Dale, B. Kiefer, M.R. Bashir, Liver fat quantification using a multi-step adaptive fitting approach with multi-echo GRE imaging, Magn. Reson. Med. 72 (2014) 1353–1365.
[12] C. Boudinaud, A. Abergel, J. Joubert-Zakeyh, M. Fontarensky, B. Pereira, B. Chauveau, J.M. Garcier, P. Chabrot, L. Boyer, B. Magnin, Quantification of steatosis in alcoholic and nonalcoholic fatty liver disease: evaluation of four MR techniques versus biopsy, Eur. J. Radiol. 118 (2019) 169–174.
[13] T. Baum, C. Cordes, M. Dieckmeyer, S. Ruschke, D. Franz, H. Hauner, J.S. Kirschke, D.C. Karampinos, MR-based assessment of body fat distribution and characteristics, Eur. J. Radiol. 85 (2016) 1512–1518.
[14] H. Donato, M. Franca, I. Candelaria, F. Caseiro-Alves, Liver MRI: from basic protocol to advanced techniques, Eur. J. Radiol. 93 (2017) 30–39.
[15] P. Bannas, H. Kramer, D. Hernando, R. Agni, A.M. Cunningham, R. Mandal, U. Motosugi, S.D. Sharma, A. Munoz del Rio, L. Fernandez, S.B. Reeder, Quantitative magnetic resonance imaging of hepatic steatosis: validation in ex vivo human livers, Hepatology 62 (2015) 1444–1455.
[16] L.A.J. Young, C.D.L. Ceresa, F.E. Mozes, J. Ellis, L. Valkovic, R. Colling, C.C. Coussios, P.J. Friend, C.T. Rodgers, Noninvasive assessment of steatosis and viability of cold-stored human liver grafts by MRI, Magn. Reson. Med. 86 (2021) 3246–3258.
[17] S.K. Satapathy, H.C. Gonzalez, J. Vanatta, A. Dyer, W. Angel, S.S. Nouer, M. Kocak, S.K. Kedia, Y. Jiang, I. Clark, N. Yadak, N. Nezakagtoo, R. Helmick, P. Horton, L. Campos, U. Agbim, B. Maliakkal, D. Maluf, S. Nair, H.H. Halford, J.D. Eason, A pilot study of ex-vivo MRI-PDFF of donor livers for assessment of steatosis and predicting early graft dysfunction, PLoS One 15 (2020) e0232006.
[18] S. Bonekamp, A. Tang, A. Mashhood, T. Wolfson, C. Changchien, M.S. Middleton, L. Clark, A. Gamst, R. Loomba, C.B. Sirlin, Spatial distribution of MRI-Determined hepatic proton density fat fraction in adults with nonalcoholic fatty liver disease, J. Magn. Reson. Imag. 39 (2014) 1525–1532.
[19] R.B. Merriman, L.D. Ferrell, M.G. Patti, S.R. Weston, M.S. Pabst, B.E. Aouizerat, N.M. Bass, Correlation of paired liver biopsies in morbidly obese patients with suspected nonalcoholic fatty liver disease, Hepatology 44 (2006) 874–880.
[20] K.N. Vu, G. Gilbert, M. Chalut, M. Chagnon, G. Chartrand, A. Tang, MRI-determined liver proton density fat fraction, with MRS validation: comparison of regions of interest sampling methods in patients with type 2 diabetes, J. Magn. Reson. Imag. 43 (2016) 1090–1099.
[21] G. Chen, J. Jiang, X. Wang, M. Yang, Y. Xie, H. Guo, H. Tang, L. Zhou, D. Hu, I.R. Kamel, Z. Chen, Z. Li, Evaluation of hepatic steatosis before liver transplantation in ex vivo by volumetric quantitative PDFF-MRI, Magn. Reson. Med. (2020).
[22] N. Bastati, D. Feier, A. Wibmer, S. Traussnigg, C. Balassy, D. Tamandl, H. Einspieler, F. Wrba, M. Trauner, C. Herold, A. Ba-Ssalamah, Noninvasive differentiation of simple steatosis and steatohepatitis by using gadoxetic acid-enhanced MR imaging in patients with nonalcoholic fatty liver disease: a proof-of-concept study, Radiology 271 (2014) 739–747.
[23] C.D. Hines, A. Frydrychowicz, G. Hamilton, D.L. Tudorascu, K.K. Vigen, H. Yu, C.A. McKenzie, C.B. Sirlin, J.H. Brittain, S.B. Reeder, T(1) independent, T(2) (*) corrected chemical shift based fat-water separation with multi-peak fat spectral modeling is an accurate and precise measure of hepatic steatosis, J. Magn. Reson. Imag. 33 (2011) 873–881.
[24] C.A. Campo, D. Hernando, T. Schubert, C.A. Bookwalter, A.J.V. Pay, S.B. Reeder, Standardized approach for ROI-based measurements of proton density fat fraction and R2* in the liver, AJR Am. J. Roentgenol. 209 (2017) 592–603.
[25] C.W. Hong, T. Wolfson, E.Z. Sy, A.N. Schlein, J.C. Hooker, S. Fazeli Dehkordy, G. Hamilton, S.B. Reeder, R. Loomba, C.B. Sirlin, Optimization of region-of-interest sampling strategies for hepatic MRI proton density fat fraction quantification, J. Magn. Reson. Imag. 47 (2018) 988–994.

[26] D. Cao, M. Li, Y. Liu, H. Jin, D. Yang, H. Xu, H. Lv, J. Liu, P. Zhang, Z. Zhang, Z. Yang, Comparison of reader agreement, correlation with liver biopsy, and time-burden sampling strategies for liver proton density fat fraction measured using magnetic resonance imaging in patients with obesity: a secondary cross-sectional study, BMC Med. Imag. 22 (2022) 92.

[27] B. Wildman-Tobriner, M.M. Middleton, C.A. Moylan, S. Rossi, O. Flores, Z.A. Chang, M.F. Abdelmalek, C.B. Sirlin, M.R. Bashir, Association between magnetic resonance imaging-proton density fat fraction and liver histology features in patients with nonalcoholic fatty liver disease or nonalcoholic steatohepatitis, Gastroenterology 155 (2018) 1428–14235, e2.

[28] J.P. Kuhn, D. Hernando, A. Munoz del Rio, M. Evert, S. Kannengiesser, H. Volzke, B. Mensel, R. Puls, N. Hosten, S.B. Reeder, Effect of multipeak spectral modeling of fat for liver iron and fat quantification: correlation of biopsy with MR imaging results, Radiology 265 (2012) 133–142.